Supplementary Materials S1

Broad-scale surface and atmospheric conditions during large fires in south-central Chile

David B. McWethy, René Garreaud, Andrés Holz, Gregory T. Pederson

Figure S1. Comparison of monthly versus seasonal fire composites. Active minus inactive monthly (panel a) and seasonal (panel b) composites of 850 hPa (about 1500 m ASL) air temperature (colors) and wind vectors (gray arrows). The largest arrows represent a wind speed difference of 4 ms-1. The letter H indicates the center of the anticyclonic anomaly, the curved black arrows indicate the area with marked easterly anomalies and the white rectangle covers south-central Chile (Valparaíso to Los Ríos districts).
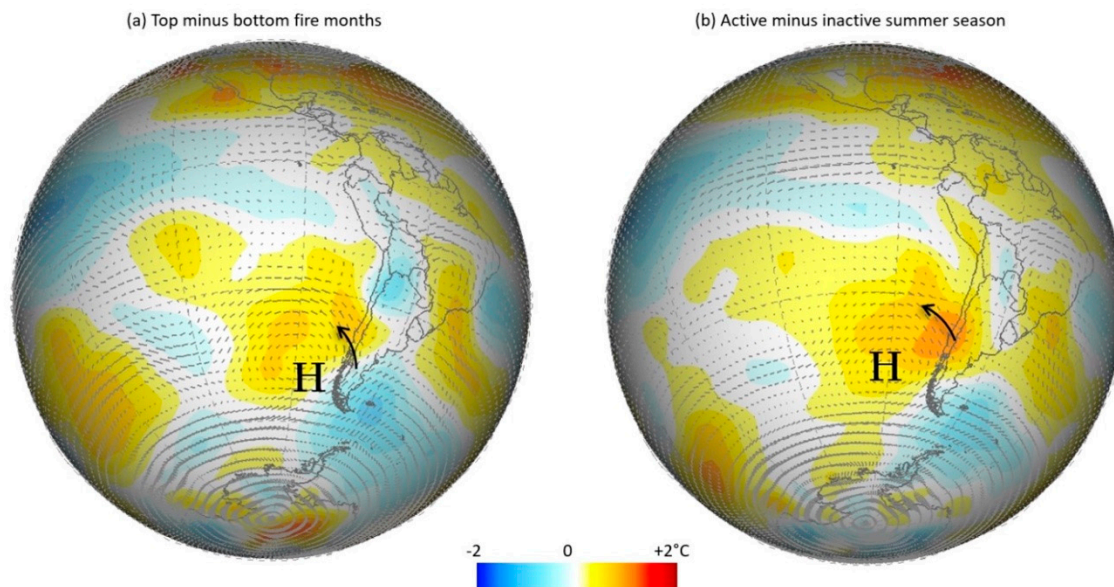

(a) Top minus bottom fire months

(b) Active minus inactive summer season

-2   0   +2°C

Figure S2. Annual area burned (AAB) correlation matrix. Correlation matrix showing Pearson correlations between annual area burned time series between regions. Regions are arranged geographically from north to south. Only significant ($p < 0.05$) correlations plotted with stronger correlations in darker colors.
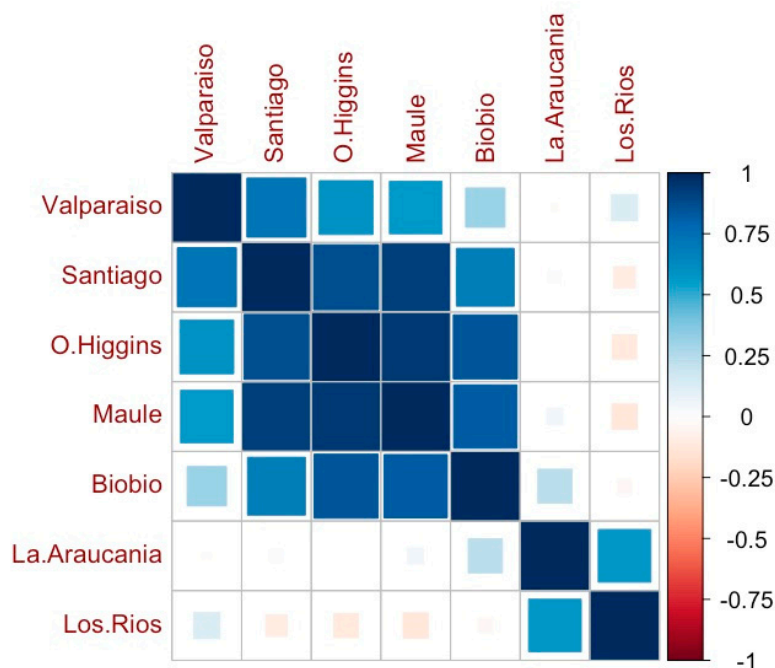
Figure S3. Climate and annual area burned (AAB) time series. Time series showing total area burned for central Chile (log scale,1000 ha), summer mean temperature (°C), winter precipitation for central Chile (mm), and summer precipitation for southern Chile (mm).
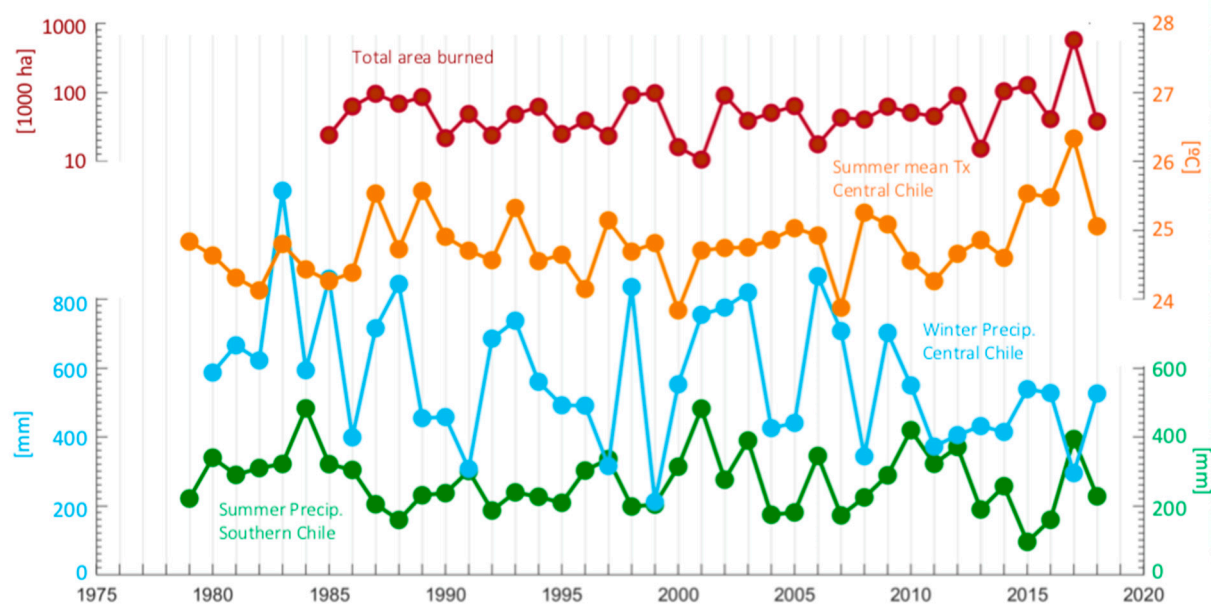
Figure S4a. Annual area burned (AAB) trend analysis. Parametric (ordinary least squares, OLS) and non-parametric (Theil–Sen) trend estimation for weighted mean fire area burned excluding the record-breaking 2016–2017 fire season (1984–**2015**) (Theil 1950, Sen 1968). Results are similar for total fire area burned but are not shown.
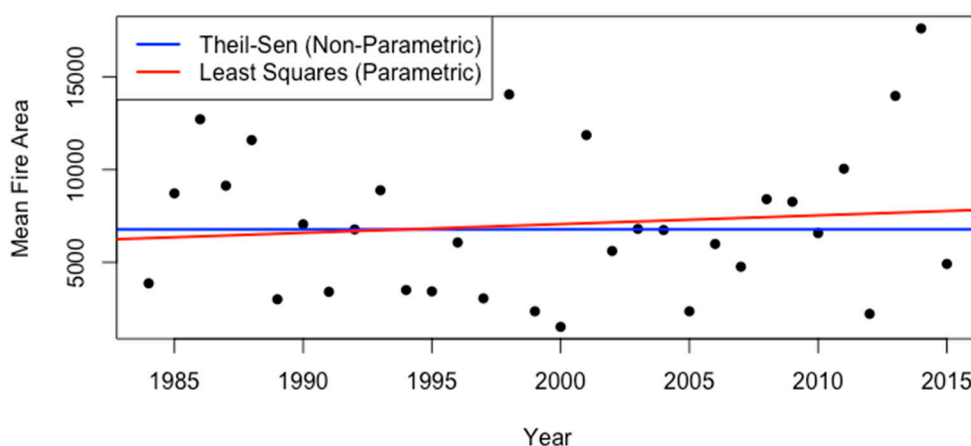

Figure S4b. Annual area burned (AAB) trend analysis. Parametric (OLS) and non-parametric (Theil–Sen) trend estimation for weighted mean fire area burned for the entire time series (1984–**2017**) (Theil 1950, Sen 1968). Results are similar for total fire area burned but are not shown.
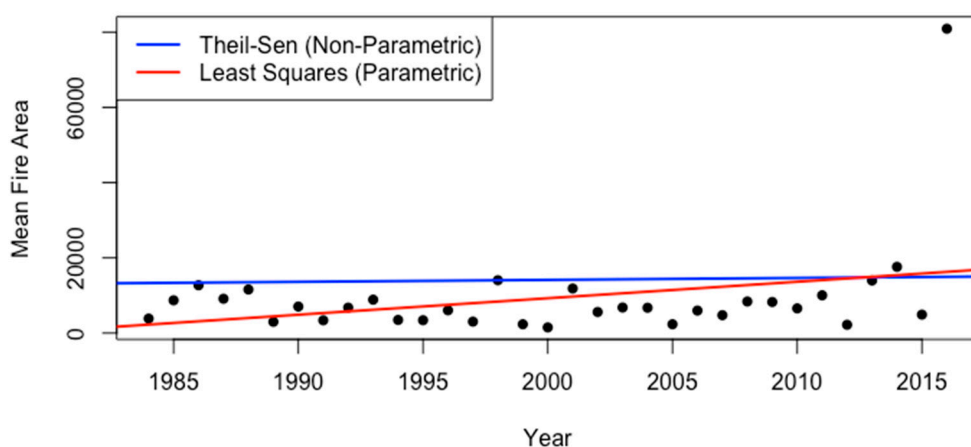
Figure S5a-d. Active fire months and El Niño–Southern Oscillation (ENSO) and Southern Annular Mode (SAM) anomalies. Departures (SDs) from mean values for monthly observed indices of ENSO (panels a,c) (MEI; (Wolter and Timlin 2011)) and SAM (panels b, d) (Marshall 2003) for a 2-month window (t − 2 to t + 2) centered on active (a, b) and passive (c, d) fire months for the entire study area (n = 20 for active fire months, n = 20 for passive fire months). Black bars indicate statistically significant (derived from 10,000 Monte Carlo simulations) departures (p < 0.1). Note different scales of the y-axes.
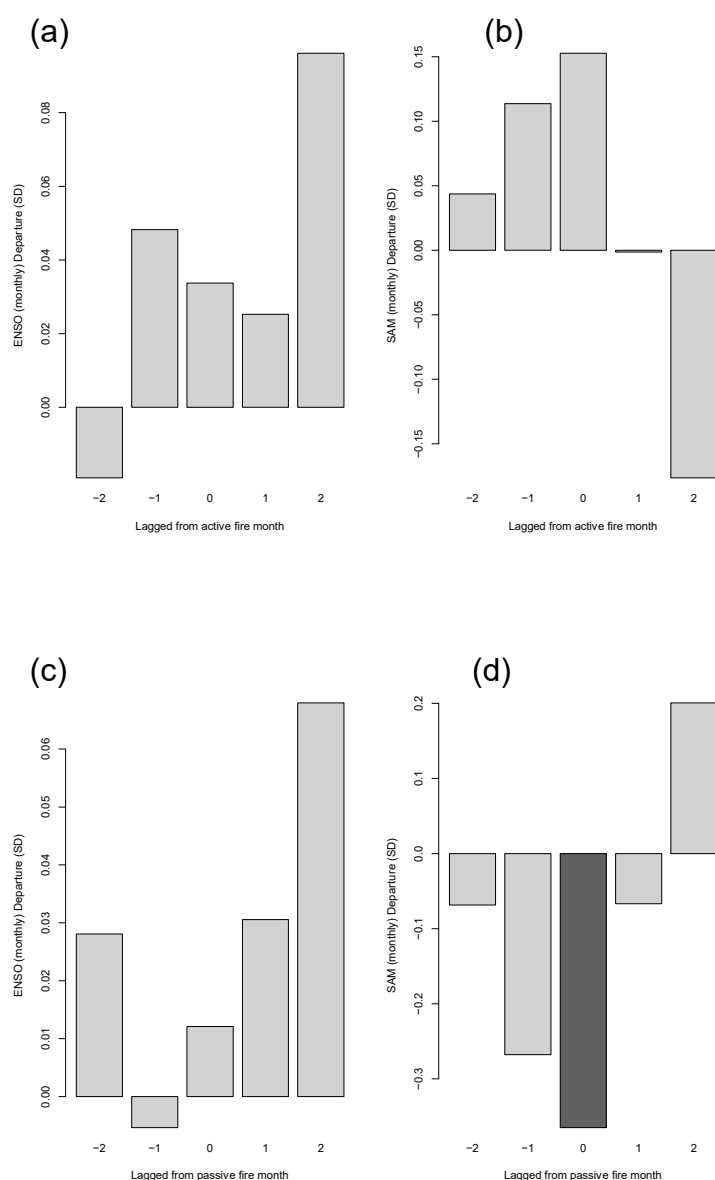
Figure S6. Difference in atmospheric subsidence between active and inactive fire months. Difference in the vertical velocity field (omega at the 500 hPa level) between active and inactive fire months.
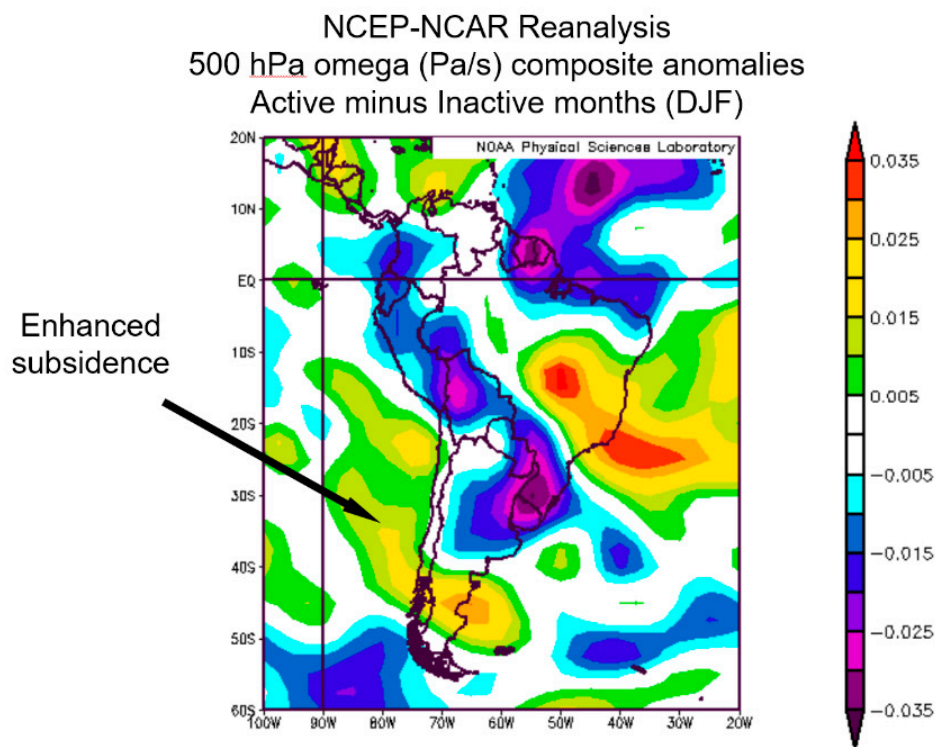
Table S1. Fire season monthly area burned summary. Summary of area burned by month for fire time series (1984-2001, top panel) and (2002–2018, bottom panel) from the Corporación Nacional Forestal of Chile (CONAF) fire dataset, all values in hectares (CONAF 2020). Red cells indicate active fire months and green cells indicate inactive fire months. FSAB = total fire season (Nov–Mar) area burned.

Fire Year	84–85	85–86	86–87	87–88	88–89	89–90	90–91	91–92	92–93	93–94	94–95	95–96	96–97	97–98	98–99	99–00	00–01
November	637	883	270	1216	946	1231	822	271	2624	4470	1264	1383	2151	168	1503	1375	428
December	3814	10,133	2920	2746	8307	1418	7647	2013	4080	7116	5483	14221	1433	1065	6052	2809	1636
January	6694	33,304	16,805	21,785	52,680	7533	6161	5272	16,763	22,840	5607	12,061	8027	11,187	34,813	7151	2824
February	7730	10,259	32,173	23,136	12,608	7044	29,758	12,963	19,491	14,521	4893	7777	6275	73,889	51,765	1813	2439
March	4833	7101	42,036	18,780	9916	4241	3627	3091	4514	12163	7331	3084	5164	3622	2247	2723	3136
FSAB	23,708	61,679	94,203	67,664	84,456	21,467	48,015	23,610	47,473	61,109	24,579	38,525	23,050	89,931	96,380	15,871	10,463

Fire Year	01–02	02–03	03–04	04–05	05–06	06–07	07–08	08–09	09–10	10–11	11–12	12–13	13 – 14	14–15	15–16	16–17	17–18
November	1856	1754	2186	503	1273	537	1380	1549	911	791	1246	1156	2364	938	857	27,698	2310
December	9904	2896	11562	8929	3369	4815	2825	7100	16,522	12,354	49,544	2001	19,854	3573	3430	34,912	5036
January	30,785	19,250	14,382	20,412	5040	31,864	11,505	32,206	26,159	9791	19,530	3983	68,285	36,359	6871	493,214	13,815
February	45,909	8782	18,446	29,228	5317	2652	17,422	10,266	3752	16,839	14,885	4280	4051	54,842	17,176	7954	10,246
March	905	5530	3309	3316	2439	2492	6774	10,191	2765	4697	3301	3652	7768	30,085	12,183	3492	5997
FSAB	89,359	38,212	49,884	62,388	17,439	42,361	39,907	61,312	50,109	44,472	88,505	15,072	102,322	125,796	40,516	567,270	37,404

References Cited

CONAF. 2020. Incendios forestales. Estadísticas históricas.

Marshall, G. J. 2003. Trends in the Southern Annular Mode from Observations and Reanalyses. Journal of Climate **16**:4134-4143.

Sen, P. K. 1968. Estimates of Regression Coefficient Based on Kendall's tau. J. Am. Stat. Ass. **63**:1379-1389.

Theil, H. 1950. A rank invariant method for linear and polynomial regression analysis. Nederl. Akad. Wetensch. Proc. Ser. A. **53**:386-392 (Part I), 521-525 (Part II), 1397-1412 (Part III).

Wolter, K., and M. S. Timlin. 2011. El Niño/Southern Oscillation behaviour since 1871 as diagnosed in an extended multivariate ENSO index (MEI.ext). International Journal of Climatology **31**:1074-1087.